Journal of Sound and Vibration (2000) **229**(3), 529–548
doi:10.1006/jsvi.1999.2494, available online at http://www.idealibrary.com on IDEAL®

ROBUSTNESS OF OPTIMAL DESIGN SOLUTIONS TO REDUCE VIBRATION TRANSMISSION IN A LIGHTWEIGHT 2-D STRUCTURE, PART II: APPLICATION OF ACTIVE VIBRATION CONTROL TECHNIQUES

D. K. ANTHONY AND S. J. ELLIOTT

Institute of Sound and Vibration Research, University of Southampton, Highfield, Southampton S017 1BJ, England

(*Received* 8 *October* 1998, *and in final form* 14 *July* 1999)

This is the second paper which considers the reduction of the vibration transmission along a lightweight cantilever structure consisting of 40 rigidly joined beams over a frequency band. In the first paper [1] the reduction was achieved by allowing the geometry of the structure to be altered, such that the structure provided an inherently better vibration isolation. In this paper, the variation reduction over a band of frequencies is achieved using feedforward active vibration control (AVC) techniques applied to the original structure geometry. The success of AVC depends strongly on the position of the actuators. The actuator positions on the structure which achieve the best reductions in vibration transmission are found for one, two and three actuators. A robustness analysis is then performed to show the sensitivity of each of the best solutions to small geometric perturbations. These solutions are the most practical, being less sensitive to small geometric changes that might occur, for example, as manufacturing tolerances. This is achieved by aplying a sufficient number of random perturbations to determine the statistical distribution of the performance. A probability limit is then applied in order to predict a likely average minimum performance criterion. In addition to considering the robustness of the performance, the control effort required to achieve active control must be considered. If this increases significantly when the structure is perturbed the demand may not be met be a practical system, and the predicted performance cannot be obtained.

1. INTRODUCTION

Unwanted vibrations have many undesirable effect in structures. This paper is the second companion paper concerned with the reduction of the transmission of vibration in a lightweight structure. Passive optimization techniques were considered in Part I of the paper [1]. In this paper a different techniques is used: that of active control of vibration (AVC). Whereas the passive optimization is strictly applicable to reducing the vibration transmission at the design stage, the application of AVC for this purpose is applicable to both the design stage and as

0022-460X/00/030529 + 20 $35.00/0

a post-design "add-on" to an existing structure. Finding the optimal actuator positions is one part of the practical optimization problem, which in itself can be demanding. Previous work [2, 3] has considered the highly combinatorial task of finding optimum actuator positions on structures to reduces vibration, or its effects. Reference [4] details the use of such methods for static shape control of a lightweight space structure. However, all the optimal solutions found by such methods may not be *practical* solutions if, in their application, the parameters cannot be guaranteed to be *exactly* the same as those specified in the solution obtained from the optimization process.

In the optimization studied here the search space is a discrete set of solutions; the possible number of actuator combinations which can become large for more than a few actuators. For each combination of actuators the maximum reduction of the vibration transmission is partially dependent on the mechanical coupling between the actuators and the region of concern and hence on the geometry of the structure. Finding the best actuator positions relies on ranking the candidates on their performance. However, if small changes to the geometry occur in service then the vibration reduction achieved can vary drastically, and the best actuator positions may not be those actually predicted by the ranking on performance of the nominal structure. A robustness analysis is performed on structures with the best ranked actuator positions in order to find the best structure in terms of a statistical measure of the performance for a percentage of random perturbations.

The structure used in this study in a two-dimensional (2-D) lightweight cantilever structure comprising 40 rigidly joined beams, organized as 10 periodic bays (see Figure 1 in the companion paper [1], where the structure is described in detail). The unwanted base vibration of the structure is represented as a transverse beam force in one of the beams at the base.

This paper is structured as follows: section 2 describes the application of active vibration control to the structure and the derivation of the cost function used, section 3 discusses how the best performance ranked sets of actuator positions were obtained. In section 4 the robustness of these actuator positions is studied. The robustness of the control effort required to achieve the AVC performance for these actuator positions is also studied. The conclusions drawn from the work are presented in section 5, Appendix A gives further details on the AVC model used.

2. ACTIVE CONTROL OF VIBRATION AND APPLICATION TO STRUCTURE

Active control of vibration (AVC) was applied to the structure in order to reduce the vibration of rightmost end beam (beam 40) of the structure. The AVC is assumed to be a feedforward implementation with each frequency considered separately, and hence there are no causality constraints. Feedforward control is especially suited to tonal vibrations and their related harmonics, where the source of unwanted vibration may be a fan or gyroscope motor, for example. It is also possible to use this control strategy for broadband disturbances [5]. Feedforward control requires a coherent reference of the vibration source which is not subject to feedback from the control actuators. In the scenario considered here, the source of vibration disturbance is modelled as a force applied to one of the beams near the

base of the structure, whilst the reference signal is assumed to be independently available from the source. Such a signal may be attained using a tachometer, for example. As in Part I the parameter reduced is the energy level in the end beam. The energy level arises from the continuous dissipation of power within the beam, which occurs due to the damping properties of the beam and the net flow of energy into the beam. In most applications of AVC the square of a quantity is used (e.g. velocity) and the formulation of the cost function in this case is well known [6]. The use of power as a cost function is becoming more widely used; for example in reference [7] the power was used as a cost function for vibration isolation and power radiation. Pan and Hansen [8] demonstrate that the use of acceleration as an estimate of power flow in a beam is very inaccurate with the near field of a source and this equally applied to structural discontinuities, such as joints. Brennan *et al.* [9] studied difference power-based control strategies (to either minimize input power to a beam or maximize secondary source output power) with the aim of reducing power transmission along a beam. The best strategy was found to be dependent upon whether the beam length was finite or infinite.

The energy level of the beam is simply related to the net power dissipated within the beam. The cost function for the net power dissipated in the beam is first derived, and then the average energy level is deduced. In the model of an active control system used here the double-acting axial operating actuators are used. For simplicity, it is assumed that the addition of an actuator to a beam does not alter the mechanical properties of that beam. The point of application of the forces from the actuators are offset (by 10 mm) from the ends of the beams.

The base vibration is modelled as a single transverse force of 1 N applied at the middle of one of the beams adjoined to the base (as shown in Figure 1 in the companion paper [1]). In AVC terminology this is called the *primary force*. Two vectors defining the effect of the force and velocity components at the joints of the ends of beam 40, in the absence of any other forces (i.e., without active control operative), are denoted by $\mathbf{f}_p$ and $\mathbf{v}_p$. AVC applies *secondary forces* to "counter" vibrations on the structure. Their effect is defined by a vector describing the values of secondary forces of each actuator $\mathbf{f}_s$, and either a "transformed" force or mobility transfer matrix ($\mathbf{C}$ or $\mathbf{Y}$) which represents the resultant force a velocity components from these secondary forces at the joints at the ends of the beam 40. More detailed information on the form of $\mathbf{C}$ and $\mathbf{Y}$ is a given in Appendix A. The net force and velocity vectors, $\mathbf{f}$ and $\mathbf{v}$, from the combination of both primary and secondary forces are then given by the summations of these two components, thus

$$\mathbf{f} = \mathbf{f}_p + \mathbf{C}\mathbf{f}_s. \tag{1}$$

and

$$\mathbf{v} = \mathbf{v}_p + \mathbf{Y}\mathbf{f}_s \tag{2}$$

where $\mathbf{v}_p$ is the vector of the six velocity components due to the primary force only.

At each joint end the force and velocity are totally qualified in the two-dimensional (2-D) model by two translational and one rotary components x, y and θ in the co-ordinate system as indicated in Figure 1 in reference [1]. The force

and velocity vectors ($\mathbf{f}$, $\mathbf{f}_p$, $\mathbf{f}_s$, $\mathbf{v}$, $\mathbf{v}_p$) are of the same format, which comprises of six components; the x and y direction translational forces or velocities and the moment and rotational velocity at both ends of the beam 40, end 0 and end 1.

The flexural energy level in beam 40 arises due to a net dissipation of power due to the beam damping. Proportional damping [10] is used. For harmonic vibration, the average dissipated power is defined as half of the real part of the conjugate product of the complex force and velocity vectors,

$$P = \tfrac{1}{2} \operatorname{Re} \{\mathbf{f}^{\mathrm{H}} \mathbf{v}\} \tag{3}$$

which can be more conveniently expressed in the linear form

$$P = \tfrac{1}{4} \{\mathbf{f}^{\mathrm{H}} \mathbf{v} + \mathbf{v}^{\mathrm{H}} \mathbf{f}\} \tag{4}$$

Using equations (1, 2) to express this in terms of $\mathbf{f}_s$, the independent variable for the cost function minimization is given by

$$P = \tfrac{1}{4} [\mathbf{f}_s^{\mathrm{H}} (\mathbf{C}^{\mathrm{H}} \mathbf{Y} + \mathbf{Y}^{\mathrm{H}} \mathbf{C}) \mathbf{f}_s + \mathbf{f}_s^{\mathrm{H}} (\mathbf{C}_s^{\mathrm{H}} \mathbf{v}_{\mathbf{p}} + \mathbf{Y}^{\mathrm{H}} \mathbf{f}_p) + (\mathbf{f}_p \mathbf{Y} + \mathbf{v}_p \mathbf{C}) \mathbf{f}_s + \mathbf{f}_p^{\mathrm{H}} \mathbf{v}_p + \mathbf{v}_p^{\mathrm{H}} \mathbf{f}_p]. \tag{5}$$

This is written in a general quadratic form as

$$J = \mathbf{x}^{\mathrm{H}} \mathbf{A} \mathbf{x} + \mathbf{x}^{\mathrm{H}} \mathbf{b} + \mathbf{b}^{\mathrm{H}} \mathbf{x} + c. \tag{6}$$

The positive scalar c represents the value of the cost function due to the primary excitation only (without active control; $\mathbf{x} = 0$). The term $\mathbf{x}^{\mathrm{H}} \mathbf{A} \mathbf{x}$ represents the value of the cost function due to the secondary source excitation only (without primary source of structural excitation), and this is obviously always positive (unless there is an external power input into beam 40). Based on these physical grounds $\mathbf{A}$ will always be positive definite. This is verified in practice by confirming that all the eigenvalues of $\mathbf{A}$ are positive. Thus, the solution to equation (6) is thus a quadratic minimum for all cases, as long as no actuator exists on beam 40, and the solution will always minimize the power dissipation in this beam. The AVC system is *overdetermined* (there are more degrees of freedom (d.o.f.s) for sensors than actuators), $\mathbf{A}$ is of full rank, thus a minimum will always exist. The minimization of the quadratic form in equation (6) is detailed in many texts, see reference [11] for example. This yields the optimum secondary control vector

$$\mathbf{x}_{\mathbf{o}} = -\mathbf{A}^{-1} \mathbf{b} \tag{7}$$

and, therefore, the optimum secondary force vector is

$$\mathbf{f}_{s_e} = -(\mathbf{C}^{\mathrm{H}} \mathbf{Y} + \mathbf{Y}^{\mathrm{H}} \mathbf{C})^{-1} (\mathbf{C}^{\mathrm{H}} \mathbf{v}_p + \mathbf{Y}^{\mathrm{H}} \mathbf{f}_p). \tag{8}$$

The minimized value of the dissipated power is of the form [11]

$$J_0 = c - \mathbf{b}^{\mathrm{H}} \mathbf{A}^{-1} \mathbf{b}. \tag{9}$$

Hence, the minimum net dissipated power is explicitly

$$P_0 = \tfrac{1}{4}\left[(\mathbf{f}_p^{\mathrm{H}}\mathbf{v}_p + \mathbf{v}_p^{\mathrm{H}}\mathbf{f}_p) - (\mathbf{f}_p^{\mathrm{H}}\mathbf{Y} + \mathbf{v}_p^{\mathrm{H}}\mathbf{C})\,(\mathbf{C}^{\mathrm{H}}\mathbf{Y} + \mathbf{Y}^{\mathrm{H}}\mathbf{C})^{-1}\,(\mathbf{C}^{\mathrm{H}}\mathbf{v}_p + \mathbf{Y}^{\mathrm{H}}\mathbf{f}_p)\right]. \quad (10)$$

This can be expressed in the more computationally efficient form as

$$P_0 = \tfrac{1}{2}\,\mathrm{Re}\,\{\mathbf{f}_p^{\mathrm{H}}\mathbf{v}_p\} - \tfrac{1}{8}\,(\mathbf{f}_p^{\mathrm{H}}\mathbf{Y} + \mathbf{v}_p\mathbf{C})(\mathrm{Re}\,\{\mathbf{C}^{\mathrm{H}}\mathbf{Y}\})^{-1}\,(\mathbf{C}^{\mathrm{H}}\mathbf{v}_p + \mathbf{Y}^{\mathrm{H}}\mathbf{f}_p). \quad (11)$$

The average energy level was used as the cost function. This is related to the dissipated power by a simple scaling factor, c_m, the beam damping which is to be independent of frequency, 20 s^{-1}. Hence the energy level of the beam is, for the general case,

$$E_{LEV}(\omega) = P(\omega)/\,c_m\,. \quad (12)$$

The average energy level over a frequency band, $\bar{E}$, is used as the parameter which is minimized by the chose of the positions of the actuators, and is given by

$$\bar{E} = \frac{1}{n}\sum_{k=1}^{n} E_{LEV}\,(\omega_L + (k-1)\,\Delta\omega), \quad (13)$$

where n is the number of frequency steps, $\Delta\omega$ the angular frequency spacing and ω_L the lower angular frequency point. $\Delta\omega/2\pi$ is 5 Hz for all cases considered in this paper.

The *total control effort* required to achieve the AVC reductions is taken to be the sum of the squares of the individuals secondary forces. The total control effort, $\bar{q}_s$, is then formally

$$\bar{q}_s = \sum_{k=1}^{n} \mathbf{f}_s^{\mathrm{H}}\,(\omega_L + (k-1)\,\Delta\omega)\mathbf{f}_s(\omega_L + (k-1)\,\Delta\omega), \quad (14)$$

where the definitions for equation (13) apply. The total control effort gives an indication of the relative electrical power required by a practical AVC system for each optimal solution presented. It does not represent the vibrational power delivered to, or dissipated by, the actuators.

3. SELECTION OF OPTIMAL ACTUATOR POSITIONS

The success of the application of AVC depends strongly on the actuator positions used. The physical reasons for this were discussed in section 2, in terms of the dynamic mechanical "coupling" between the primary forces and the secondary actuators and the end beam. The average energy level over the frequency band 150–250 Hz was used as the parameter to be minimized in this paper (see equation (13)). This corresponds to maximizing the average attenuation of this parameter, though in the field of AVC it is far more common to refer to the performance improvement in this sense. The frequency band comprises 21 equally spaced frequency points 5 Hz apart from 150 to 250 Hz, the same as those used for

broadband optimization for the passive structure which was studied in the companion paper [1]. That total control effort was also calculated for each case. The control effort was evaluated for a 1 N transverse primary force and has the units of N^2. If the primary force were increased the control effort would increase in proportion to the square of the primary force.

The optimum actuator positions were sought for the application of AVC using one, two and three actuators. This was achieved by an exhaustive testing of all possible combinations of actuators positions, for each number of actuators. Beam 40 was not considered as a candidate position (as explained in section 3). Hence for one, two and three actuators there are 39, 741 and 9139 possible combinations respectively. Because combinations and not premutations are sought it is important that the algorithm generating the candidate actuator positions does not produce and then discard repeated combinations. This would be very wasteful and would affect the run time of such algorithms by a factor of 36! for the three actuator case, for example. Even if the cost function were not evaluated in repeated combinations the formulation of all the permutations would be still very expensive, and can dominate the optimization evaluation time. The best 10 single actuator positions of AVC systems having one, two and three actuators are shown in Figures 1, 2 and 3 respectively. These are shown from the top in order of decreasing attenuation, the value of which is denoted along with the total control effort for each single actuator position.

Figure 1 shows the 10 best positions for one actuator, for which the range of attenuation is 10·8–8·5 dB. The actuator positions do not appear to follow any particular rule; positions at the extreme ends of the structure are included in the best 10. A general rule of thumb in active control is to treat the unwanted vibration nearest to its place of origin. This does not seem to bear out in the case of best ranked 10 candidates. One of the actuators is, however, on the same beam as the external vibration is introduced. The secondary actuator produces an axial force whilst the external primary force is, however, in the transverse direction.

The total control effort required to achieve each level of attenuation (for the primary force used) is also shown in Figure 1. There is a large range of values ranging from 1400 to 17 200. This illustrates the fact that the choice of candidate must be made on the basis of both attenuation achievable and total control effort required. The second-best ranked candidate is likely to be the position chosen in practice since it has good control performance and a low control effort.

Figures 2 and 3 show the 10 best candidates for two and three actuators respectively. For two actuators the achievable values of attenuation range from 31·1 to 26·9 dB, with total control effort ranging from 11 000 to 53 900. Here the third ranking set of actuator locations appears to be a good practical choice since it has good control performance and a low control effort. For three actuators, the range of achievable values of attenuation is 50·8–44·0, dB, and the total control effort range is 24 400–244 000. This range is large due to one "rogue" set of actuator locations with a particularly high value of control effort. With two actuators, there again appears to be no particular rule in the placement of the actuators for the best 10 AVC set of actuator positions. However, the actuator positions chosen are found to be only in the first seven leftmost structure bays. This trend in seen to continue

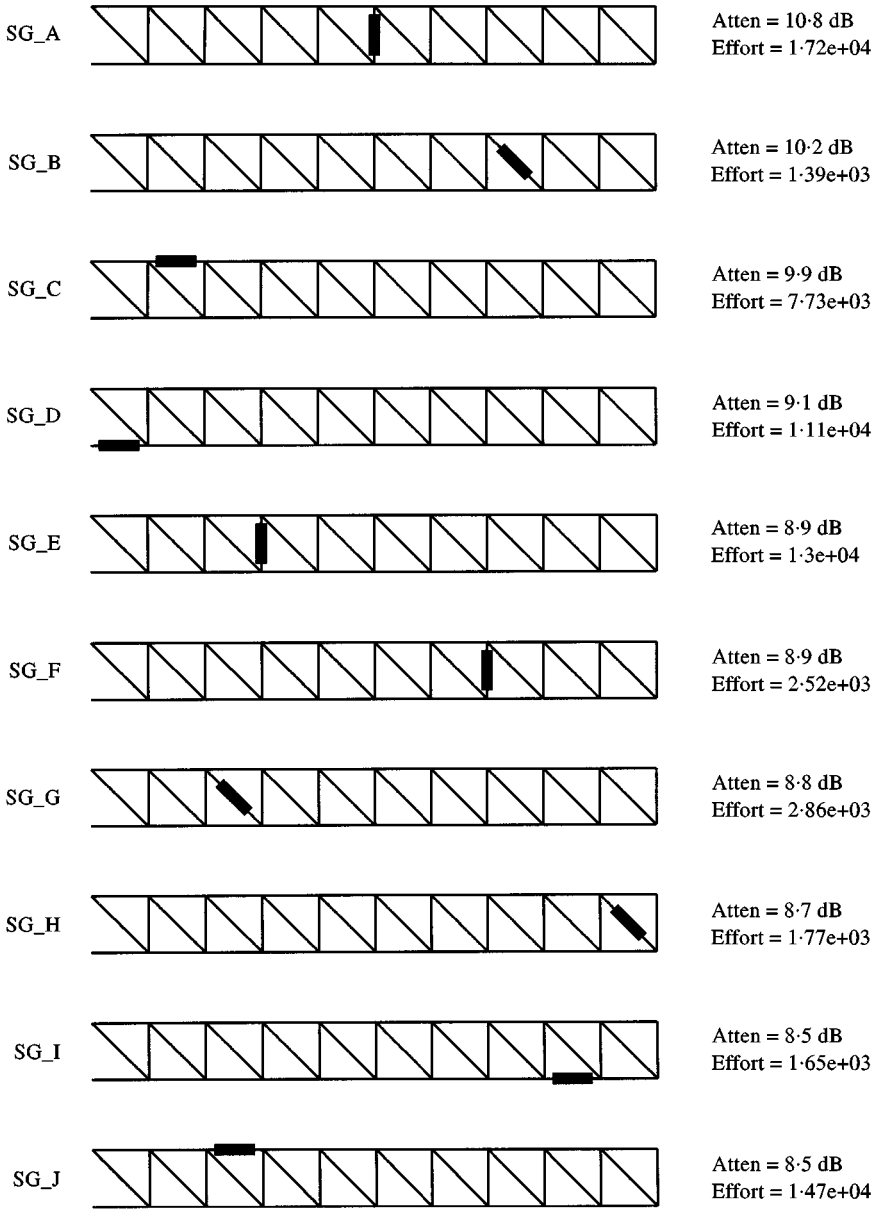

Figure 1. The 10 best performance ranked single-actuator positions for the frequency band 150–250 Hz.

for the three actuator case, the actuators now only appearing in the five leftmost structure bays; the left-half of the structure.

Figure 4 shows the best 10 actuators position for four actuators. This case is not considered any further in this paper since the high levels of attenuation shown (up to about 119 dB) would not be achievable in practice using a control system with a realistic noise floor. However, the inclusion of these results does demonstrate the trend further, that the larger the number of actuators the more the actuator

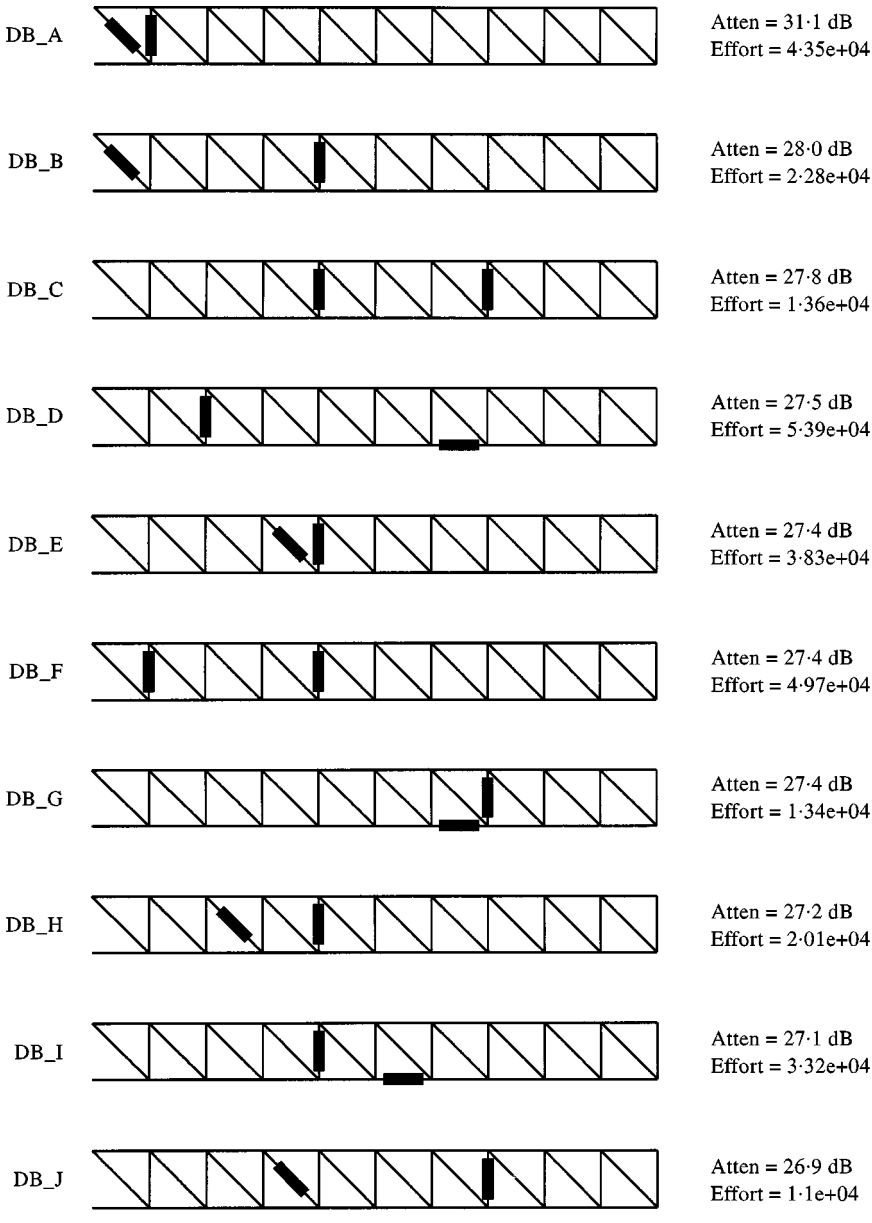

Figure 2. The 10 best performance ranked two-actuator positions for the frequency band 150–250 Hz.

position are found to be closer to the primary excitation at the base of the structure. Here the actuators are restricted to the four leftmost bays. Furthermore, the best five sets of actuator positions were found to only use actuator positions in the three leftmost structure bays.

The effective "total control effort" of the primary force is 21 N^2, since the primary force at each frequency is 1 N. It is interesting to note that the control effort required by the AVC system is much larger is all cases. The smallest control effort of

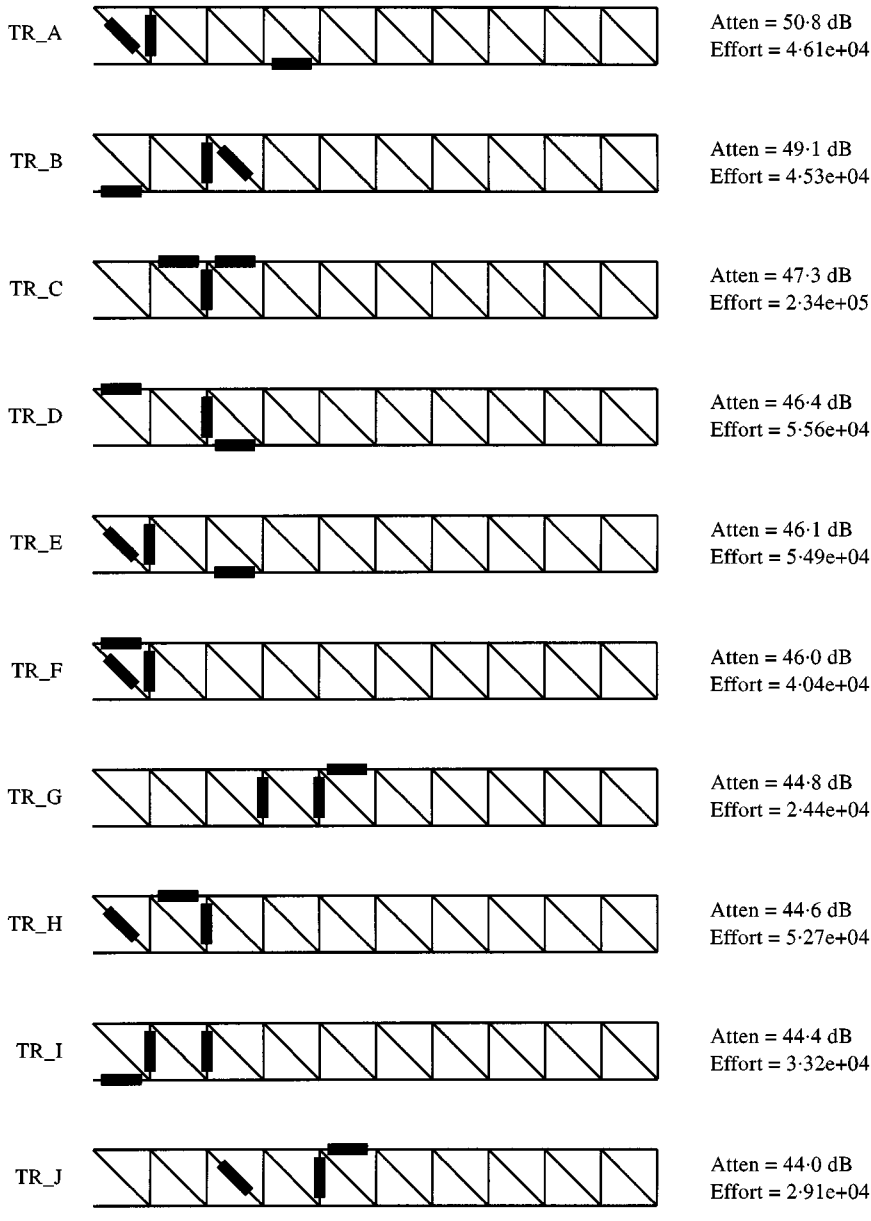

Figure 3. The 10 best performance ranked three-actuator positions for the frequency band 150–250 Hz.

all the optimal positions presented is for the single actuator position SG_B, and is greater by a factor of over 60.

The value of attenuation achieved in the performance of the structures shown in Figures 1–4 is that of the frequency band average attenuation, as described in equation (13). Within the band various levels of attenuation are achieved at individual frequencies. Figure 5 shows the attenuation response at the 21 individual frequencies considered, for the application of AVC with actuators positions DB_A

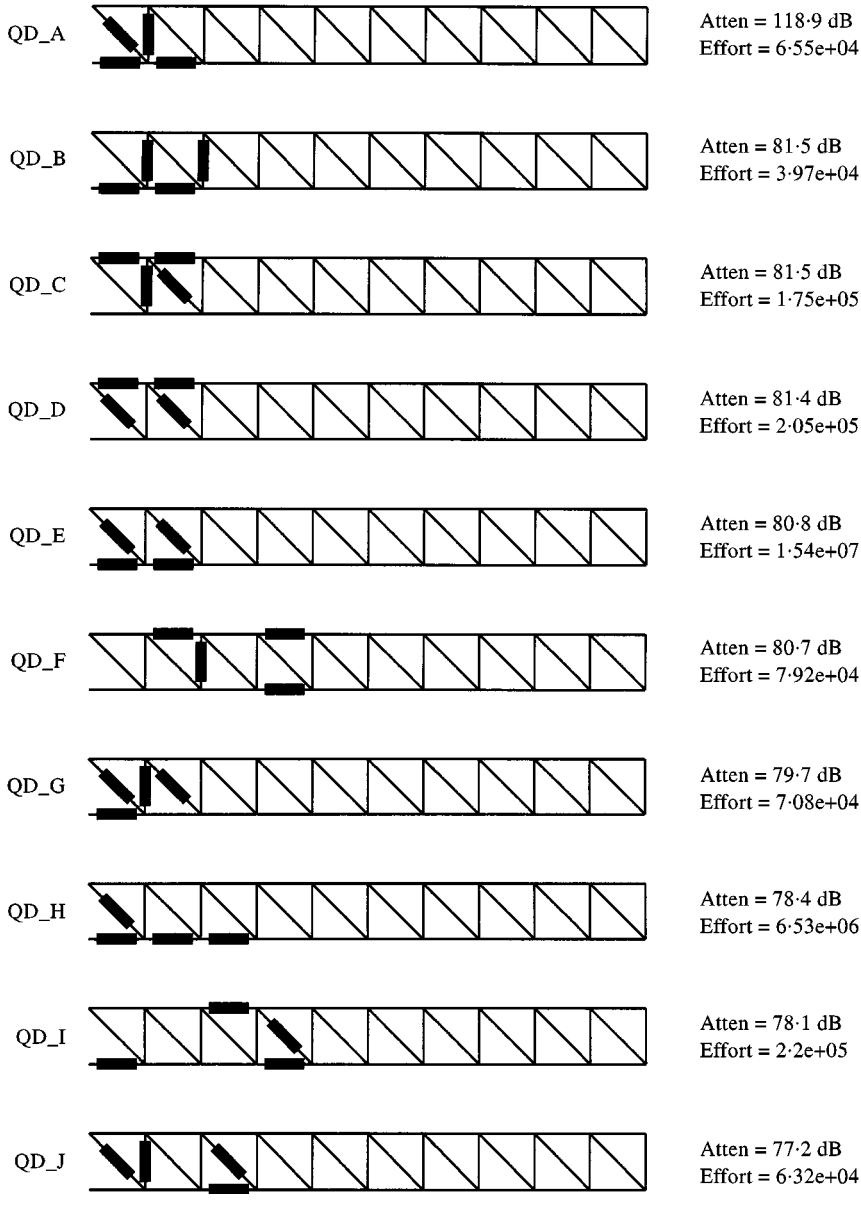

Figure 4. The 10 best performance ranked four-actuator positions for the frequency band 150–250 Hz.

(in Figure 2). Since a feedforward control strategy is used, the AVC system has no effect on the performance of the vibrational energy in beam 40 outside the band of frequencies controlled.

Comparing the vibrational energy reduction achieved by both the passive optimization (detailed in the Part I) and active optimization (using AVC), it is found that the application of AVC with two actuators produces magnitudes of reductions similar to those of passive case [1]. Whilst in Figure 1–3 the reductions

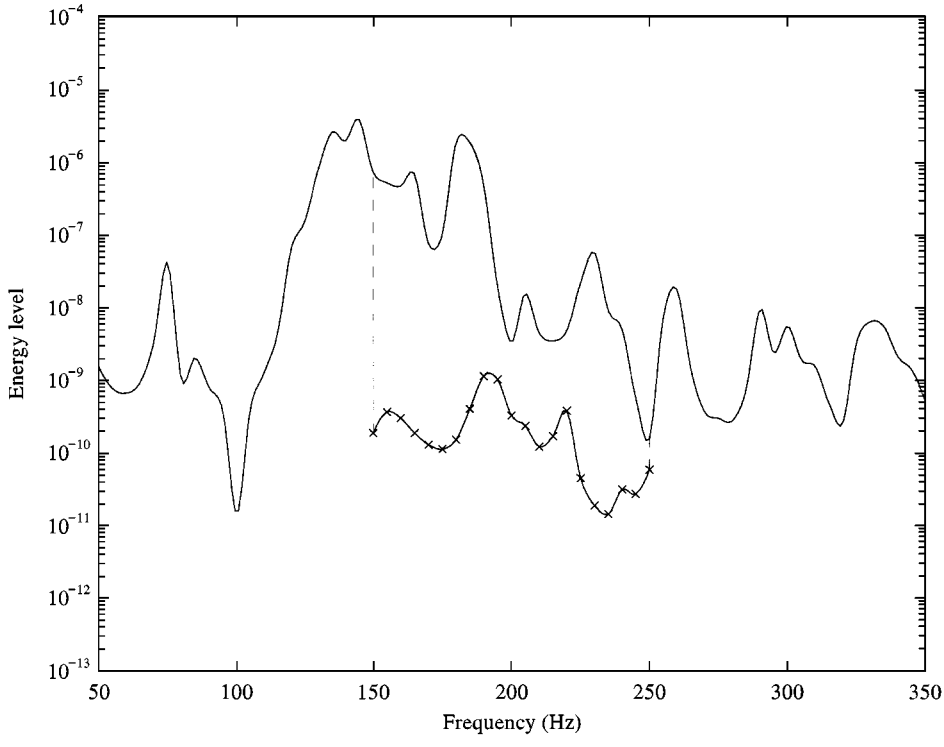

Figure 5. Frequency response of the structure without AVC (——), and reduced response obtained with AVC (-×-×-×-), within frequency band applied, for actuator positions DB_A in Figure 2.

in vibration are given in decibels, but in the next section, Figure 6, for example, shows the vibration reductions with a non-decibel scale, allowing the vibration reductions obtained to be easily compared with Figures 7 and 11 in the companion paper [1].

4. STUDY OF ROBUSTNESS OF ACTUATOR POSITION COMBINATIONS

The study of the robustness of the performance of the various actuator positions to geometric perturbations was performed in order to determine which of the candidates is more practical to implement. The same set of 300 perturbations was applied to the structure as used for the robustness analysis of the passively optimized structures in reference [1]. The perturbations are uniformly distributed between $\pm$ 10 mm and are applied to both the x and y co-ordinates of each of the middle 18 joints of the structure. The robustness analysis is only applied to the two- and three-actuator positions sets, as these systems are most likely to be used in practice.

In the robustness of the passively optimized candidates the geometric perturbations change the mechanical impedance between the externally applied force and ends of beam 40. This directly affects the average energy level in beam 40. However, in the optimization considered in this paper is a discrete one; the

solutions are sets of actuator positions. These best 10 actuator positions are chosen on the basis of a ranking of the nominal (unperturbed) performance. When the system undergoes perturbations the achievable attenuation is re-evaluated is order to show how well the actuator positions originally chosen with the nominal structure perform under such geometric perturbations.

Evaluating the perturbed performance of an AVC system in this manner corresponds to applying the AVC system to a real structure where manufacturing tolerances are the perturbations from the nominal design. It is also assumed that the controller has an accurate model of the plant [11 Chapter 5]. If the plant were to change over periods comparable or less than the update period of the plant model, the AVC system would be operating with an inaccurate model of the plant. This could be due to geometric changes of the structure caused by significant changes in the static load, or may be through thermal expansion and contraction. The perturbation analysis performed here is not intended to cover robustness under these conditions. These perturbations are likely to be structured, and the perturbations to each joint position could no longer be treated independently, as in this analysis. The robustness of the control performance and effort for the two- and three-actuator systems have been evaluated.

Figures 6 and 7 show the results of the perturbation analysis for the values of achievable attenuation for each of the best 10 ranked two- and three-actuator AVC

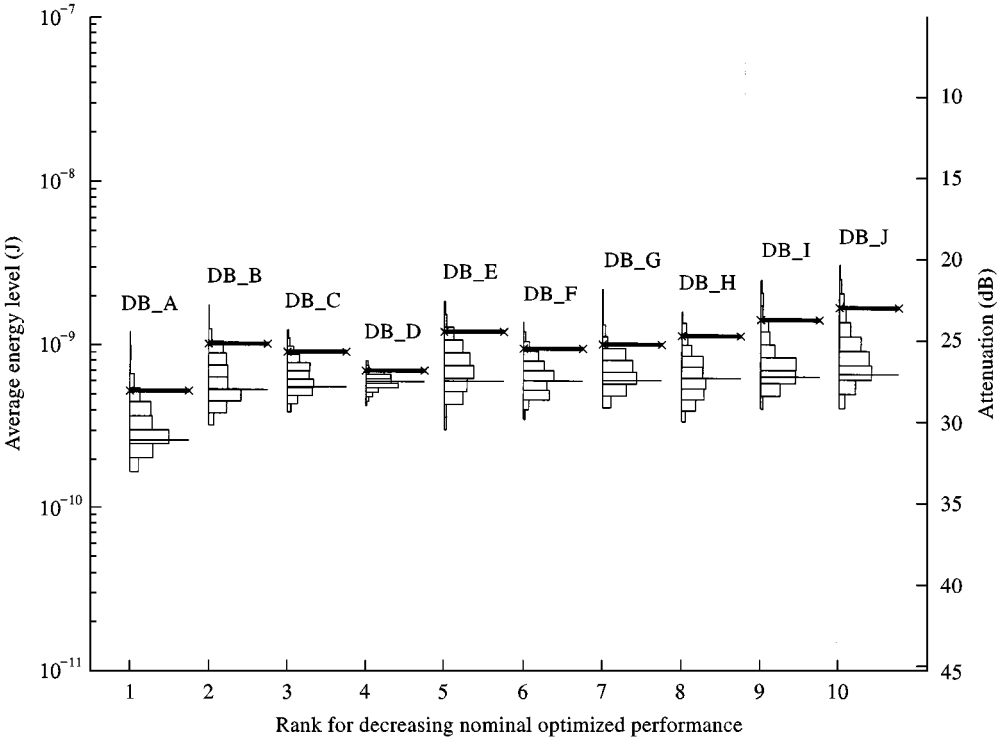

Figure 6. Statistical distribution and 95% probability limits for the AVC performance, for frequency band 150–250 Hz, of the 10 best ranked two-actuator positions.

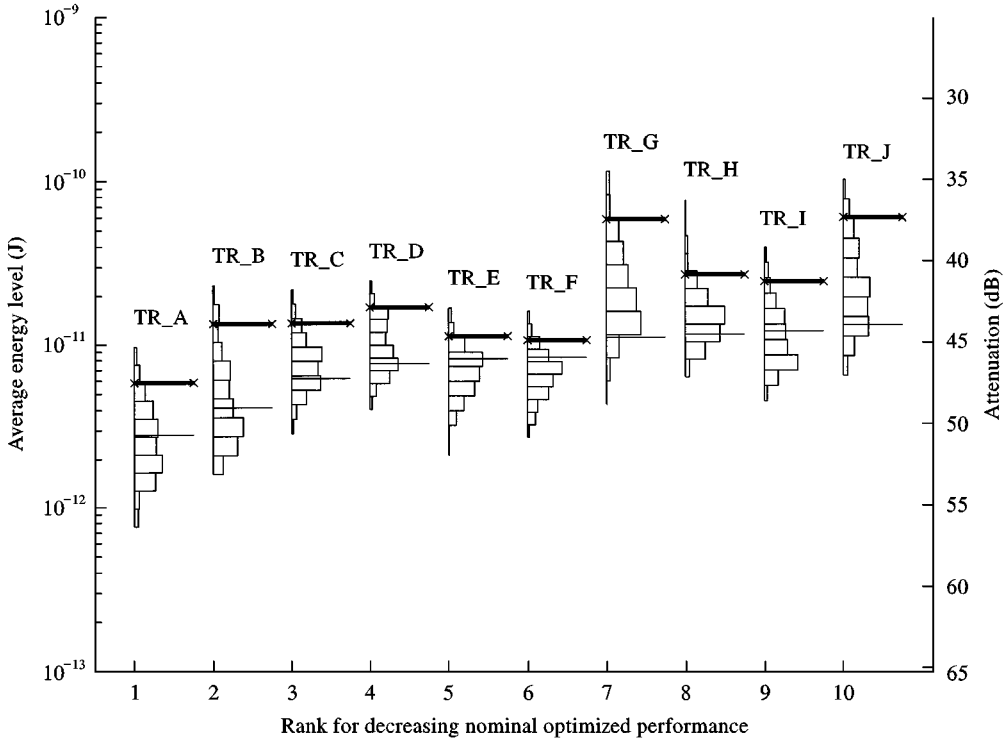

Figure 7. Statistical distribution and 95% probability limits for the AVC performance, for frequency band 150–250 Hz, of the 10 best ranked three-actuator positions.

actuator positions (ranked on nominal performance). The results are also summarized in Tables 1 and 2. The figures consist of histograms showing the statistical distribution of the minimized energy level in beam 40.

The results for each structure are displayed in order of ranking under nominal conditions, the value of which is represented by the this solid line on each histogram. The 95% probability limit is shown by a solid bold line. This indicates the value of of minimized energy level which, for the 300 experiments performed, is less or equal than this value for 95% for all perturbations. The 300 perturbations used were found to be sufficient to find the "shape" of the distribution, and hence this will be an estimate of the actual 95% limit. The graphs show the reduced vibration energy level with logarithmic axes as in Figure 11 in the Part I for the perturbation analysis for the passively optimized structures to facilitate comparison between the two optimization cases. In the field of AVC, it is more common to deal with value of attenuation express in decibels; a second y-axis on the right is included for this purpose.

Considering first the two actuator AVC actuator positions in Figure 6 it is seen that DB_D is the most robust candidate, for which the entire spread of the statistical distribution is about 3 dB, while most of the other actuator positions appear to have a statistical spread of about 10 dB. Using three actuators, Figure 7, it is seen that the majority of the distributions have a range of one order of

TABLE 1

Results summary for AVC using best performance ranked two-actuator positions over bandwidth 150–250 Hz

Structure	Nominal attenuation (dB)	95% probability limit attenuation (dB)	Nominal control effort (N^2)
DB_A	31·1	28·1	43500
DB_B	28·0	25·2	22800
DB_C	27·8	25·6	13600
DB_D	27·5	26·8	53900
DB_E	27·4	24·4	38300
DB_F	27·4	25·4	49700
DB_G	27·4	25·2	13400
DB_H	27·2	24·6	20100
DB_I	27·1	23·6	33200
DB_J	26·9	22·9	11000

TABLE 2

Results summary for AVC using best performance ranked three-actuator positions over bandwidth 150–250 Hz

Structure	Nominal attenuation (dB)	95% probability limit attenuation (dB)	Nominal control effort (N^2)
TR_A	50·8	47·6	46100
TR_B	49·1	43·9	45300
TR_C	47·3	43·9	224000
TR_D	46.4	42·9	55600
TR_E	46.1	44.7	54900
TR_F	46·0	44·9	40400
TR_G	44·8	37·5	24400
TR_H	44·6	40·9	52700
TR_I	44·4	41·3	33200
TR_J	44·0	37·4	29100

magnitude with a few, notably actuator positions TR_G & TR_J, whose distribution spread approaches 20 dB. In general, the three-actuator positions achieve reductions of 15–20 dB better than those with two actuators. If robustness alone is the primary consideration then DB_D is the best two-actuator position. There is no obvious "best choice" for the three-actuator positions in terms of robustness.

Considering the 95% probability limit a selection of the actuator positions may be made in terms of both robustness and absolute performance. For 95% of perturbations the performance is equal to or better than the value of the 95%

probability limit. In most applications the minimum reduction is the important factor. For the two-actuator positions the choice of nominally well-ranked positions DB_B and DB_C becomes less favourable. It is also seen that there is little difference in performance between DB_A and DB_D in terms of this criterion, but the latter is more robust, and even the worst perturbed performance is better than the majority of the perturbed performance values for DB_A. This set of actuator positions is also seen to have a small probability of having much poorer performance than the 95% limit. Considering the 95% probability limit for the three-actuator positions, it is seen that the nominally best ranked actuator position is also the best choice with this criterion.

There is another consideration in applying AVC apart from the achieved performance: the control effort required to achieve this. There will be a limit on the control effort with a practical system, either individual actuator effort or total system effort. In general, AVC actuator positions with smaller required control effort are preferable. It is possible to augment the cost function used here in the ranking of each AVC actuator position, with a term to penalize positions with higher control efforts and produce a bias towards lower control effort solutions. This was implemented [12], but was not considered here, since it would unnecessarily complicate the study. Robustness analysis should, however, also consider the control effort. As the structure is perturbed the control effort required is likely to change even if the performance is insensitive to such changes, if the control effort increases significantly above its nominal value then a practical system may not be able to maintain the predicted vibration reduction. This is avoidable if the increase is predicted and the demand remains feasible.

Figures 8 and 9 show the results of a robustness analysis on the total control effort for the best 10 two- and three-actuator positions, with same format as in Figure 6. The same perturbations as before were used. It is reiterated that the scale used on the graph is logarithmic, and that a factor of over 5 exists between the nominal control effort for TR_B and TR_C, for example, which emphasizes the importance of the consideration of control effort. It is seen that for both two- and three-actuator systems the range of total control effort, both nominal and perturbed, are similar even though the three-actuator case produces larger reductions of the vibration. In general, it is seen that there is less diversity in the robustness of the control effort that with the performance. However, the cost of increased control effort is often realized in linear terms, and the absolute value of the control effort is important. Actuator arrangement DB_D, which is favoured in terms of its performance is seen to require, for 95% of the perturbation cases, about four times more total control effort than DB_C. The compromise of performance and control effort will vary depending on the application. Considering the three-actuator positions, results it is seen that TR_C, whilst well ranked in terms of performance, is particularly costly in terms of control effort. Initially, TR_F may seem to be a "bad choice" due to the large spread of the distribution. However, it is apparent that the "rogue" high value of control effort arises from the results of only one perturbation, and if this particular perturbation value had not appeared in the set of 300 perturbations then this set of actuator positions would appear more robust. This justifies the use of a 95% probability limit, and not simply the worst

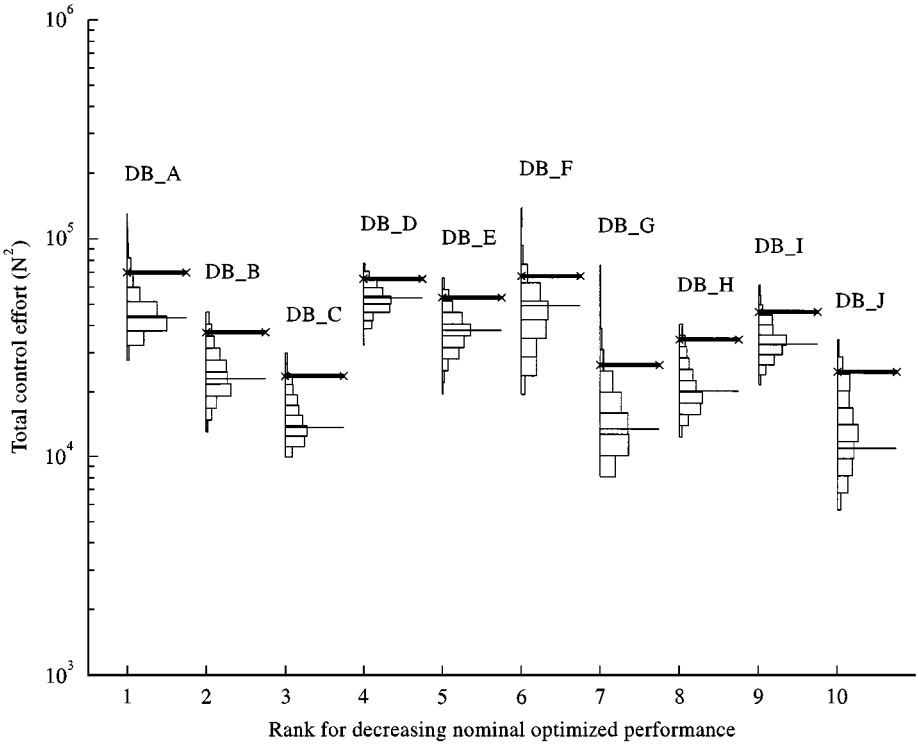

Figure 8. Statistical distribution and 95% probability limits for the AVC total control effort, for frequency band 150–250 Hz, of the 10 best ranked two-actuator positions.

case. Indeed, using the 95% probability limit, TR_F is ranked third in terms of the minimum expected control effort.

Hence, for an AVC system, it is necessary to consider both the performance and control effort when considering robustness. Each set of actuator positions can be robust in terms of performance, total control effort, or both. When ranked in terms of nominal performance the more *performance robust* a set of actuator positions is, the more likely its ranking will remain high in terms of the 95% probability limit. However, *control effort robustness* is also important if the application is to be realized practically.

5. CONCLUSIONS

Feedforward active vibration control (AVC) was applied in a simulation study to a lightweight cantilever structure in order to reduce the vibration transmission from the base to a beam at the end of the structure. The parameter minimized was the energy level within the end beam of the structure, averaged over 150–250 Hz. The optimization problem considered was to find the actuator positions that achieve the greatest reductions in vibration. This was done by exhaustive search, since, this is feasible in this case even though the total number of possible combinations increases rapidly with number of actuators used. AVC systems using

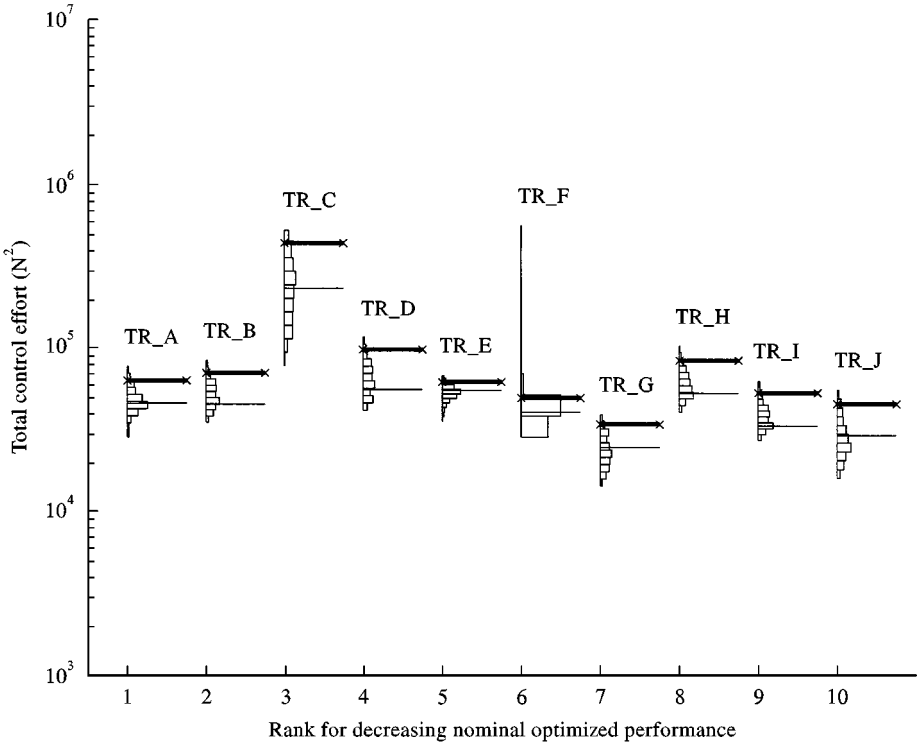

Figure 9. Statistical distribution and 95% probability limits for the AVC total control effort, for frequency band 150–250 Hz, of the 10 best ranked three-actuator positions.

up to four actuators were considered, although the robustness analysis was only extended to the two- and three-actuator cases. These produced realistic and practically achievable reductions. Using a two-actuator AVC system, similar reductions were obtained as with the passive optimization used in the first paper. An AVC system operating with any of the optimal actuator positions presented requires a control effort much larger than the equivalent control effort of the unwanted vibration souce. The optimal actutor position with the smallest control effort is still over fifty times greater than that of the vibration source itself.

The robustness of the 10 best-ranked AVC actuator positions on the structure for one to three actuators was then studied, in order to find the positions which are more practical in the sense of being more resistant to small changes in the structure geometry. As in Part I, this was achieved by applying a set of random perturbations enabling the statistical distribution of a performance to be obtained. Another consideration, other than the performance, which must be considered in the application of AVC is that of the control effort required to achieve the predicted vibration reductions. This may be a consideration when choosing the best solution under nominal conditions and could be incorporated into the optimization search. However, under structural perturbations, the control effort is seen to increase by factors over 10 times for some AVC actuator arrangements. If the control effort is not considered and under structural perturbations it is seen to rise beyond the

capabilities of a practical system then the predicted performance (nominal or robust) will not be realized. Hence, for AVC systems, there are two types of robustness; *performance robustness* and *control effort robustness*. A 95% probability limit was applied to performance and control effort statistical distributions obtained from the perturbations applied. This is the basis for determining the worse value (for performance or control effort), which will only be violated for an estimated 5% of perturbation instances (assuming the same perturbation distribution).

A further companion paper is planned in which the vibration transmission of the structure studied here is minimized by using both passive methods (or geometric redesign, as in reference [1]) and active methods (AVC system using optimally placed actuators).

ACKNOWLEDGMENTS

The first author acknowledges support in the form of a studentship from the Faculty of Engineering & Applied Science at The University of Southampton.

REFERENCES

1. D. K. Anthony, S. J. Elliott and A. J. Keane *Journal of Sound and Vibration*. Robustness of optimal design solutions to reduce vibration transmission in a lightweight 2-D structure. Part I: Geometric redesign (submitted).
2. H. Furuya and R. T. Haftka 1996 *Journal of Spacecraft & Rockets* **33**, 422–427. Combining genetic and deterministic algorithms for locating actuators on space structures.
3. M. T. Simpson and C. H. Hansen 1996 *Noise Control Engineering Journal* **44**, 169–184. Use of genetic algorithms to optimise vibration actuator placement for active control of harmonic interior noise in a cylinder with floor structure.
4. S. Hakim and M. B. Fuchs 1996 *American Institute of Aeronautics and Astronautics Journal* **34**, 1505–1511. Quasistatic optimal actuator placement with minimum worst case distortion criterion.
5. J. S. Vipperman, R. A. Burdisso and C. R. Fuller 1993 *Journal of Sound and Vibration* **166**, 283–299. Active control of broadband structure vibration using the LMS adaptive algorithm.
6. C. R. Fuller, S. J. Elliott and P. A. Nelson 1996 *Active Control of Vibration*. London: Academic Press.
7. O. Bardou, P. Gardonio, S. J. Elliott and R. J. Pinnington 1997 *Journal of Sound and Vibration* **208**, 111–151. Active power minimisation and power absorption in a plate with force and moment excitation.
8. X. Pan and C. H. Hansen 1993 *Journal of Sound and Vibration* **165**, 497–510. The effect of error sensor location and type on active control of beam vibration.
9. M. J. Brennan, S. J. Elliott and R. J. Pinnington 1995 *Journal of Sound and Vibration* **186**, 657–688. Strategies for the active control of flexural vibration on a beam.
10. F. S. Tse, I. E. Morse and R. T. Hinkle 1978. *Mechanical Vibrations. Theory and Applications*. Boston, MA: Allyn and Bacon, Inc.
11. P. A. Nelson and S. J. Elliott 1992 *Active Control of Sound*. London: Academic Press.
12. K. H. Baek and S. J. Elliott 1995 *Journal of Sound and Vibration* **186**, 245–267. Natural algorithms for choosing source locations in active control systems.

APPENDIX A: FORMULATION OF PLANT MATRICES

The two "transformed" plant matrices used in the main text, **C** and **Y**, are themselves comprised of two terms, so equations (1) and (2) may be written as

$$\mathbf{f} = \mathbf{f}_p + \mathbf{C}'\,\mathbf{T}\mathbf{f}_s, \tag{A1}$$

$$\mathbf{v} = \mathbf{v}_p + \mathbf{Y}'\,\mathbf{T}\mathbf{f}_s, \tag{A2}$$

where $\mathbf{C}'$ and $\mathbf{Y}'$ are the force transfer and mobility transfer matrices, which define the mechanical coupling between the actuators and their effect on the force and velocity components at the ends beam 40. **T** is a transformation matrix which maps each axial secondary force onto six components in each plant matrix. This is required because the force and velocity components at the end of beam 40 are not independent in all d.o.f.s, but are solely defined by the axial forces of the force vector, $\mathbf{f}_s$.

For two secondary force actuators, equation (A1) is then

$$\begin{bmatrix} \begin{Bmatrix} f_x^{40,0} \\ f_y^{40,0} \\ f_\theta^{40,0} \end{Bmatrix} \\ \begin{Bmatrix} f_x^{40,1} \\ f_y^{40,1} \\ f_\theta^{40,1} \end{Bmatrix} \end{bmatrix} = \begin{bmatrix} \begin{Bmatrix} f_{p_x}^{40,0} \\ f_{p_y}^{40,0} \\ f_{p_\theta}^{40,0} \end{Bmatrix} \\ \begin{Bmatrix} f_{p_x}^{40,1} \\ f_{p_y}^{40,1} \\ f_{p_\theta}^{40,1} \end{Bmatrix} \end{bmatrix}$$

$$+ \begin{bmatrix} \begin{Bmatrix} \mathbf{C}_{1A}^{40,0} \\ \mathbf{C}_{1A}^{40,1} \end{Bmatrix} & -\begin{Bmatrix} \mathbf{C}_{1B}^{40,0} \\ \mathbf{C}_{1B}^{40,1} \end{Bmatrix} & \begin{Bmatrix} \mathbf{C}_{2A}^{40,0} \\ \mathbf{C}_{2A}^{40,1} \end{Bmatrix} & -\begin{Bmatrix} \mathbf{C}_{2B}^{40,0} \\ \mathbf{C}_{2B}^{40,1} \end{Bmatrix} \cdots \end{bmatrix} \begin{bmatrix} \{\mathbf{1}\} & & \\ & \{\mathbf{1}\} & \\ & & \ddots \end{bmatrix} \begin{bmatrix} f_{s_1} \\ f_{s_1} \\ \vdots \end{bmatrix} \tag{A3}$$

where, for example, $f_x^{40,0}$ is the x-axis force component at end 0 of beam 40. The submatrices in the $\mathbf{C}'$ matrix are of the format

$$\mathbf{C}_{1A}^{40,0} = \begin{bmatrix} c_{1A_x}^{40,0} & 0 & 0 \\ 0 & c_{1A_y}^{40,0} & 0 \\ 0 & 0 & c_{1A_\theta}^{40,0} \end{bmatrix}, \tag{A4}$$

where $c_{1A_x}^{40,0}$ is the individual force transfer function for the x-axis force component at end 0 of beam 40 for a unit axial force at one end (A) of the beam where the first secondary actuator is employed. This notation is extended to responses in the y-axis, rotational components; from end B of the actuator beam position; and for end 1 of beam 40. The signs of the submatrices for a secondary drive from end B are negative to give the proper representation of a double-acting actuator. The reason for the diagonal form of the submatrices is to ensure that all the net force and net

velocity components remain independent and only combined in the final inner product between **f** and **v** so that the power flow components from the six d.o.f.s are summed and not the force or velocity components.

The $\{\mathbf{1}\}$ submatrices in equation (A3) are vectors which are explicitly

$$\{\mathbf{1}\} = (1 \;\; 1 \;\; 1 \;\; 1 \;\; 1 \;\; 1)^{\mathrm{T}} \tag{A5}$$

and map a single value for each secondary actuator onto the all six individual transfer function it relates to. For convenience, the force transfer matrix and the transformation matrix are combined to form a transformed force transfer matrix **C**.

In a similar manner for **Y** is the transformed mobility transfer matrix, where the **Y**′ matrix (A2) and its submatrices are defined:

$$\mathbf{Y}' = \begin{bmatrix} \begin{Bmatrix} \mathbf{Y}_{1A}^{40,0} & -\mathbf{Y}_{1B}^{40,0} \\ \mathbf{Y}_{1A}^{40,1} & -\mathbf{Y}_{1B}^{40,1} \end{Bmatrix} & \begin{Bmatrix} \mathbf{Y}_{2A}^{40,0} & -\mathbf{Y}_{2B}^{40,0} \\ \mathbf{Y}_{2A}^{40,1} & -\mathbf{Y}_{2B}^{40,1} \end{Bmatrix} & \cdots \end{bmatrix}, \tag{A6a}$$

$$\mathbf{Y}_{1A}^{40,0} = \begin{bmatrix} y_{1A_x}^{40,0} & 0 & 0 \\ 0 & y_{1A_y}^{40,0} & 0 \\ 0 & 0 & y_{1A_\theta}^{40,0} \end{bmatrix}, \tag{A6b}$$

where $y_{1A_x}^{40,0}$ is the individual transfer mobility, detailing the x-axis force component at end 0 of beam 40 for a unit axial force at end A of the beam where the first secondary actuator is employed.